DOE/ER/40374-23

BEAM-BEAM INTERACTION AND PACMAN EFFECTS IN THE SSC WITH RANDOM NONLINEAR MULTIPOLES*

G. P. Goderre†, N. K. Mahale and S. Ohnuma

DOE/ER/40374--23

DE89 013949

May 25, 1989

The University of Houston-University Park
Houston, TX 77204-5504, USA

Summary

In order to find the combined effects of beam-beam interaction (head-on and long-range) and random nonlinear multipoles in dipole mgnets, transverse tunes and smears have been calculated as a function of oscillation amplitudes. Two types of particles, "regular" and "pacman", have been investigated using a modified version of the tracking code TEAPOT. Regular particles experience beam-beam interactions in all four interaction regions (IR's), both head-on and long-range, while pacman particles interact with bunches of the other beam in one medium-beta and one low-beta IR's only. The model for the beam-beam interaction is of weak-strong type and the strong beam is assumed to have a round Gaussian charge distribution. Furthermore, it is assumed that the vertical closed orbit deviation arising from the finite crossing angle of 70 μrad is perfectly compensated for regular particles. The same compensation applied to pacman particles creates a closed orbit distortion. Linear tunes are adjusted for regular particles to the design values but there are no nonlinear corrections except for chromaticity correcting sextupoles in two families. Results obtained in this study do not show any reduction of dynamic or linear apertures for pacman particles when the oscillation amplitude is less than ∿10σ. However, smears often exhibit a strong dependence on tunes, casting some doubts on the validity of defining the linear aperture from the smear alone.

Introduction

The primary purpose of this study is to investigate the possible aperture reduction in the realistic SSC lattice caused by the long-range beam-beam interaction and an associated phenomenon called "pacman" effect. Realistic lattice means that all elements of the ring are taken into account exactly as designed and that random nonlinear multipoles with their rms values specified by the SSC Central Design Group(CDG) are assigned to each dipole magnet. (See Table 1.)

The long-range interactions between two opposing beams are unavoidable when beams cross at a small but finite angle which is taken to be 70μrad in this study. It is easy to see from a simple analytical estimate[1] that, within each low-beta IR of the SSC lattice, the long-range tune shift is approximately twice the head-on value. Equally important may be the distortion in the vertical closed orbit caused by the vertical dipole field when two beams are separated vertically as in the SSC. Although this separation generates nonlinear multipoles as well which are absent in head-on collisions, the resulting nonlinear effect such as tune spread is much less for particles with modest amplitude(i.e.,less than a few sigma of the beam size) than the similar effect in head-on collisions.

The pacman effect, named after the early video game PAC-MAN, results from the abort gap in each train of bunches.[2] The gap is ∿3 microsecond long corresponding to some 200 missing bunches. Unlike regular particles which meet bunches of the opposing beam at all possible head-on and long-range interaction points, pacman particle may encounter the abort gap in some IR's and thereby experience different beam-beam interactions. Differences that may become responsible for the effects are

1) Vertical closed orbit distortion. The distortion for regular particles can be eliminated by a suitable steering system. Since it is not easy to have an independent orbit control for pacman particles, steering adjusted for regular particles will not eliminate the orbit distortion of the pacman particles completely. Coupled with the nonlinear multipole fields in the ring magnets, this orbit distortion may be damaging to pacman particles and may even lead to their eventual loss.

2) Tune shifts. When the best working point in the tune diagram is chosen for regular particles, pacman particles will occupy an area which is in general not optimum since tune shifts arising from the overall beam-beam interactions are different for two types of particles.

3) Because of the off-center beam-beam collisions, pacman particles are subjected to odd-order resonances. If one tries to eliminate some dangerous resonances for regular particles by means of correction magnets, this correction may create adverse effects on pacman particles.

There is an inherent difficulty in trying to estimate the pacman effect in the realistic SSC lattice with random nonlinear multipoles in every dipole. It is unlikely that pacman particles will be destroyed in a few seconds or less. The working area in the tune diagram needed simultaneously for regular and pacman particles is not difficult to find when the dynamic aperture(i.e., aperture free of beam loss in $\sim 10^3$ revolutions corresponding to ∿300ms)alone is considered.[2,3] Beam loss due to pacman effect will be a rather slow one; it will be detectable in computer simulations only if the tracking covers $\sim 10^6$(still less than five minutes of the SSC beam lifetime) or more. When CRAY-XMP is used to run an existing code such as TEAPOT,[4] the required running time will be of the order of fifty hours and the reliability of results is by no means assured. The status of analytical investigation is even less encouraging. Presently available estimates of the long-term lifetime are arguably still in the realm of speculation for any practical(in contrast to idealized) situations of interest.[5] It is then necessary to set up some criteria, which can not be entirely free of arbitrariness, that must be invoked to define the phase space area of long-term stability.

The concept of "linear aperture" has been introduced by the SSC-CDG and used by them extensively in the discussion of aperture requirement. Originally, it was meant to determine the aperture within which the particle motion is "sufficiently" linear so that one can

*Work supported by the US Department of Energy under grant No. DE-FG05-87ER40374.

†Present address: Fermi National Accelerator Laboratory, P.O. Box 500, Batavia, IL 60510, USA.

Submitted to the Third Advanced ICFA Beam Dynamics Workshop,
Novosibirsk, USSR, 29 May - 3 June 1989

predict the behavior of particles wwth confidence. As such, the linear aperture was associated with the ease of machine operations, particularly for the diagonostic ones during the commissioning period. In order to make the definition quantitative, a quantity called "smear" was introduced (with not-always-agreed-upon definitions). The linear aperture is such that the value of the smear is less than 30% or 6.4%, these two values associated with two different ways of defining the smear. Over the years, the meaning of linear aperture seems to have been extended and there is definitely a wishful thinking that, since the motion is sufficiently linear within it, the linear aperture may provide the sought-after aperture for the long-term lifetime as well.

The underlying assumption in this stydy is as follows: The linear aperture defined in terms of the certain value of smear may not be the right parameter in discussing the long-term lifetime of a particle, but it is still useful in comparing two different particles. That is, if the linear aperture for the pacman particle is as large as the one for the regular particle, the pacman effect should not be significant.

In this study, tunes and smears as a function of oscillation amplitudes are shown for both regular and pacman particles when random nonlinear multipoles exist in dipole magnets and there are two low-beta and two medium-beta IR's in the ring. Tunes and smears have been obtained by processing the tracking data on (x,x',y,y') at one point in the ring. The number of revolutions is usually 2,048 but 512 and 1024 are also used in some cases. The definition of smears used here is given in Appendix.

A notion of the "stability aperture", which is different from the dynamic aperture but qualitatively similar to the linear aperture, has been proposed by Tennyson in his extensive study of beam-beam effects in the SSC.[6] His results are based on trackings of more than 150,000 revolutions.

Simulation Model and Tracking Calculation

Basic parameters of the SSC relevant to the present study are listed in Table 2. Since the beam-beam interaction is assumed to be of the weak-strong type, the closed orbit of the strong beam is kept fixed. For the given vertical crossing angle of 70μrad, the separation of two beams is found taking into account the focusing action of insertion quadrupole triplets as well as the effects of long-range beam-beam interaction. The original version of TEAPOT could not handle any vertical bend and it had to be modified to include the proper transformation of vertical coordinate system when the particle enters or leaves interaction regions. The transformation is such that the vertical closed orbit of the regular particle maintains the predetermined beam separation in each IR and no orbit distortion is created in the arc sections of the ring. As the coordinate transformation simulates the required vertical steering at the entrance and exit of each IR, the vertical closed orbit for the pacman particle is different from the one for the regular particle.

The charge distribution of the strong beam is taken to be Gaussian with a round cross section of rms size $\sigma \equiv \sqrt{\sigma_x \sigma_y}$. The beam will not be round within the quadrupole triplets but the error in the calculation of the resulting tune shift is found to be less than 10% when σ_x/σ_y is between one-half and two.[7] The magnitude of the linear tune shift due to the head-on collision is given by

$$\Delta\nu_{HO} = (N_B r_p / 4\pi\ \varepsilon_N) = 0.89\times10^{-3}$$

where N_B = number of particles in a bunch, ε_N = normalized rms emittance, and r_p = classical proton radius. This quantity is often called the linear beam-beam parameter with the symbol ξ. The tune shift itself is $-\Delta\nu$ so that the total head-on tune shift from four IR's is -3.6×10^{-3} for both directions.

When the effect of quadrupoles on the beam separation is ignored within an IR, the magnitude of long-range tune shift for particles with small oscillation amplitudes is

$$\Delta\nu_{LR} = (N_B r_p\ n/2\pi\gamma\beta^* \alpha^2) = 1.6\times10^{-3} \text{ for low-beta IR}$$

where γ = 20TeV/0.94GeV, β^* = 0.625m, α= 70μrad, and n = number of long-range encounters. With the effect of quadrupoles taken into account, there is a slight increase, from 0.0016 to 0.0020 in low-beta IR's. Since the long range tune shifts are $-\Delta_{LR}$ in the horizontal direction and $+\Delta_{LR}$ in the vertical , the overall horizontal tune shift is much larger than the vertcial one:

total from four IR's = -0.0075(H) & +0.0005(V)

A particle with initial condition (x=y,x'=y'=0) is tracked for a number of turns and its position in phase space at a fixed location in the ring is recorded for each turn. A fast Fourier transform (FFT) of the data gives horizontal and vertical tunes as a function of the amplitude. Smears are found from the quantity

$$W_x \equiv A_x^2 = (x/\sqrt{\beta_x})^2 + (\alpha_x x/\sqrt{\beta_x} + \sqrt{\beta_x}\ x')^2$$

and the similar quantity W_y evaluated at each turn. See the appendix for the expression of smear in terms of (A_x, A_y).

Since the smear is regarded as a convenient quantity to measure the degree of nonlinearity in particle motion, it should not include any direct contributions from the linear part of the motion. More specifically, A_x and A_y should be calculated with the effects of closed orbit distortion or linear coupling removed.

closed orbit: It is easy to find the closed orbit (x_c, x_c', y_c, y_c') at the observation point in the ring where A's are to be calculated at each turn if parameters such as (Δp/p) and field strengths of dipoles and quadrupoles are not modulated. The proper expression for A is obtained by replacing (x,x',y,y') with $x-x_c$, $x'-x_c'$, etc. Finding the closed orbit with a good accuracy may become a major undertaking when there are modulating parameters of the beam or the ring elements. One can recover the static picture by considering an imaginary machine which is $n = (f_{rev}/f_{mod})$ times larger. The lattice of this machine consists of n superperiods, each superperiod being identical to the original "small" machine. Because of the modulation, the true closed orbit exists only for the larger machine. Calculation of A's may require a large number of turns to be tracked since one point in (A_x,A_y) plane can be found only after every n-th turn instead of every turn for the unmodulated case.

linear coupling: In the presence of linear coupling, A_x and A_y are no longer constant of the motion and there will be a smearing when the trajectory is plotted in (A_x,A_y) plane even for a purely linear machine. One must go to (A_u,A_v) plane of the two eigenmodes U and V. Exact expressions for $W=A^2$ are given by Edwards and Teng in connection with their proposal for a parametrization of four-by-four symplectic matrix.[8] Of many cases investigated in this study, the linear coupling influence is (barely) visible only for pacman particles.

Results and Discussion

Main results of this study are displayed in Figs. 1 to 16 and in Table 3. Basic parameters used for the calculation are summarized in Table 2. The number of turns tracked is 2,048 unless otherwise stated explicitly.

Table 1.

Random magnet errors are assigned to each dipole assuming Gaussian distribution. The sigma associated with the distribution for each of the multipole components is shown in this table. These values are applicable at 20TeV excitation.

$$B_y + iB_x \equiv B_o + B_o \sum_{n=0} (b_n + ia_n)(x+iy)^n; \quad b_n \text{ normal}, \; a_n \text{ skew}$$

n	$b_n(10^{-4}\text{cm}^{-n})$	$a_n(10^{-4}\text{cm}^{-n})$	
2	0.40	0.61	(sextupole)
3	0.35	0.69	(octupole)
4	0.59	0.14	(decapole)
5	0.059	0.16	
6	0.075	0.034	
7	0.016	0.030	
8	0.021	0.0064	
9	0.003	0.0056	

(1) Average values are all assumed to be zero.
(2) Dipoles b_0 and a_0, and quadrupoles b_1 and a_1 are assumed to be effectively zero in the ring because of the expected compensation.
(3) The sigma for b_2(normal sextupole) is assumed to be achievable with the "binning" proposed by R. Talman. The actual value will be several times larger.

Table 2.

Summary of the SSC Parameters Used

Ref. "Conceptual Design of the Superconducting Super Collider", SSC Central Design Group, March 1966. Table 4.1-1, p. 95.

"Realistic lattice", with clustered IR's, 60^{o}/cell

Ring = (41 cells)+2x(42 cells)+(41 cells)+(medium-beta section)+(41 cells)+2x(42 cells)+(41 cells)+(low-beta section).

(medium-beta section)= two IR's with β^*=10m,
(low-beta section) = two IR's with β^*=0.625m.

circumference(rev. freq.)	82.944km(3614.4Hz)
bunch separation	5 m
nominal IR space (*)	free ±20 m, total ±72.5 m
number of bunch encounters (*)	58/IR
normalized rms emittance ε_N	1.0 mm-mrad
tunes (nominal)	78.265(H) & 78.285(V)
abort gap (missing bunch)	3.1 μs (≈200)

(*) These are for two low-beta IR's. The length of medium-beta IR is twice as long compared with the one for low-beta IR so that the number of bunch encounter is also twice as much.

Table 3-1

Regular particle, Q_x = 78.265 (H) & 78.285 (V)

(av. amp./σ) (H)	(av. amp./σ) (V)	(r/σ)	fractional tunes (H)	fractional tunes (V)	S_x(%)	S_y(%)	S_{rms}(%)	C_{xy}
2.21	2.19	3.11	.2671	.2871	2.4	1.9	0.28	−0.25
4.40	4.47	6.28	.2679	.2875	6.8	5.8	0.71	−0.52
7.63	7.33	10.6	.2690	.2851	14.6	9.7	1.69	−0.33
8.31	7.89	11.5	.2692	.2847	15.5	12.8	1.97	−0.08
9.20	8.28	12.4	.26955	.2843	17.5	13.3	1.89	−0.20
10.1	9.44	13.8	.2700	.28405	14.6	10.7	1.57	−0.16
18.0	16.8	24.6	.2710	.2842	12.9	8.7	1.23	−0.19
Pacman particle								
2.20	2.19	3.11	.2698	.2859	1.9	1.5	0.21	−0.22
4.39	4.44	6.25	.27005	.2861	4.6	4.4	0.46	−0.52
8.26	8.16	11.6	.2709	.2845	12.0	7.4	1.22	−0.28
10.8	10.3	14.9	.27135	.2842	16.4	7.9	2.52	+0.29
12.7	11.2	17.0	.2715	.2842	26.8	10.0	4.68	+0.56
17.4	17.3	24.6	.2717	.2843	15.0	7.1	1.88	+0.15

Table 3-2

Regular particle, Q_x = 78.267 (H) & 78.287 (V)

4.45	4.47	6.32	.2700	.2895	8.0	6.4	0.72	−0.54
6.03	5.99	8.50	.2704	.2882	12.3	10.9	1.27	−0.50
8.37	7.35	11.1	.2714	.2869	37.2	12.4	5.91	+0.40
9.70	10.9	14.6	.2719	.2860	45.3	42.8	7.92	+0.30
Pacman particle								
4.40	4.49	6.28	.2720	.28805	4.6	5.5	0.56	−0.40
5.88	5.96	8.37	.2724	.2874	7.5	6.4	0.70	−0.56
8.94	8.83	12.6	.2730	.2862	8.8	9.5	1.25	−0.08
10.5	10.3	14.7	.2733	.2861	8.7	12.6	1.65	−0.33

Regular particle, Q_x = 78.263 (H) & 78.283 (V)

4.41	4.47	6.28	.2659	.28545	6.7	5.6	0.73	−0.50
5.96	6.02	8.47	.2662	.2842	12.1	9.6	1.25	−0.55
7.81	7.36	10.7	.2671	.2829	17.5	11.0	1.50	−0.50
10.3	10.8	14.9	.2681	.28175	15.4	25.2	2.58	−0.49
Pacman particle								
4.40	4.45	6.25	.2681	.28405	5.0	4.0	0.46	−0.52
5.93	5.97	8.42	.2684	.2833	9.9	6.3	0.95	−0.36
9.04	8.89	12.7	.2690	.2822	12.8	9.4	1.61	+0.27
10.4	10.1	14.5	.2692	.2822	15.3	11.5	2.19	+0.01

Table 3-3

	Case 1	Case 2	Case 3	Case 4	Case 5
Regular particle, (av. amp./σ) = 4 for both directions.					
S_x(%)	6.8	6.2	7.1	6.4	6.6
S_y(%)	5.8	5.8	6.4	6.3	6.3
S_{rms}(%)	0.71	0.70	0.79	0.75	0.69
C_{xy}	−0.52	−0.50	−0.43	−0.45	−0.53
Regular particle, (av. amp./σ) = 10 for both directions.					
S_x(%)	29.0	30.5	33.2	NA	29.8
S_y(%)	22.7	22.6	22.6		14.0
S_{rms}(%)	2.29	2.71	3.61		3.17
C_{xy}	−0.80	−0.76	−0.67		−0.67
Pacman particle, (av. amp./σ) = 4 for both directions.					
S_x(%)	4.6	3.9	4.6	4.4	4.3
S_y(%)	4.4	4.3	4.5	4.8	4.7
S_{rms}(%)	0.46	0.46	0.56	0.52	0.49
C_{xy}	−0.52	−0.51	−0.40	−0.42	−0.50
Pacman particle, (av. amp./σ) = 10 for both directions.					
S_x(%)	16.4	16.0	NA	17.0	16.2
S_y(%)	7.9	7.4		7.9	7.3
S_{rms}(%)	2.52	2.09		2.69	2.35
C_{xy}	+0.29	+0.20		+0.32	+0.29

Fig. 1: An example of FFT fo find tunes with 2,048 turns.

Fig. 2: An example of particle trajectories in the normalized phase space. Islands are visible suggesting some high-order resonances.

Fig. 3: Fractional part of the horizontal tune as a function of the average oscillation amplitude (given in terms of the rms beam size σ_x). The tune spread for pacman particles is approximately one-half of the spread for regular particles.

Fig. 4: Same as Fig. 3, vertical tune.

Fig. 5: Horizontal smear S_x (see appendix for the definition) as a function of the average horizontal amplitude/σ_x. The abnormal increase in the smear for pacman particles starting around 10σ is a clear indication of some resonances. From this behavior, one may conjecture that the pacman effect could be important beyond ∿10σ.

Fig. 6: Smear in the vertical direction. Again there is an indication of resonances for pacman particles near the amplitude 12σ, although it is not as pronounced as in the horizontal direction.

Fig. 7: rms smear as a function of the combined amplitude (see appendix for the definition).

Fig. 8: The same trajectory as in Fig. 2 but the phase-space structure is more clearly discernible when plotted as a function of the betatron oscillaton phase ϕ:

$$\phi = \tan^{-1}\{(\beta x' + \alpha x)/x\}$$

Fig. 9: Vertical trajectory of the particle shown in Figs. 2 & 8. The phase-space structure is more complicated than in the horizontal direction, suggesting a seven-sided shape.

Fig. 10: Same as Fig. 8 but plotted as a function of the turn number.

Fig. 11: Same as Fig. 10 but the average amplitude is ∿50% of Fig. 10. Note the disappearance of the slow amplitude modulation which is in Fig. 10. The significance of this modulation is not clear.

Fig. 12: Same as Fig. 11 (av. amp.≃4σ). This clearly shows the (negative) correlation between two directions. The correlation parameter C_{xy} (see appendix for the definition) is -0.52.

Figs. 13 to 16:

These are for a pacman particle and should be compared, respectively, with Figs. 8, 9, 10, and 11.

Table 3-1 is a compilation of the main results from this study. It should be noted that the correlation parameter C_{xy} for the pacman particle changes its sign from negative to positive around amplitude≃9σ where the horizontal smear starts a rapid growth. In order to see the sensitivity of the result on the choice of tunes, slightly different values have been tried for a few cases and the results are given in Table 3-2:

Case 1. Both tunes are increased by 0.002 from the nominal design values.

Case 2. Both tunes are decreased by 0.002.

According to the definition of "linear aperture" used by the SSC Central Design Group,

$$S_{x,y} < 30\% \quad \text{or} \quad S_{rms} < 6.4\%,$$

even the variation of tunes of this magnitude may be quite significant for some cases.

Finally, Table 3-3 lists partial results with five different choices of the seed number which generates a particular distribution of multipole fields (but with the same rms values given in Table 1) around the ring. At least up to amplitude ≃ 10σ, smears and the correlation parameter are quite similar, indicating that it is not necessary to study many different cases for the present purpose.

Synchrotron Oscillation

Results of tracking calculations with synchrotron oscillations are still scanty and of a preliminary status. The model for simulating the synchrotron oscillation is a very simple-minded one: the field strenths of all magnets in the ring are modulated sinusoidally with the period 527 turns and the relative magnitude of 1.25 $\times 10^{-4}$, which is 2.5 times the expected rms energy spread of the beam at 20 TeV. Because of the modulation of the closed orbit, one must deal with a ring which is 527 times larger than the SSC ring. It is a time-consuming task to locate the exact closed orbit of this large ring and to obtain just one point in (A_x,A_y) plane after tracking 527 turns of the SSC. The total number of turns for fifty points is then 527×50=26,350 turns. If the slow rise observed in the horizontal amplitude is taken at its face value, the relative growth of amplitude is ∿4×10^{-4}/oscillation.

Various effects associated with the synchrotron oscillation in the SSC are discussed in the Conceptual Design Report.[9] One may conclude that the most important of them is the modulation of tunes which can cause many overlapping sideband resonances and they in turn may create a chaotic behavior.[10] According to Tennyson, the effect of tune modulation on the stability aperture is rather insensitive to the choice of modulation magnitudes (between ±.0007 and ±.003) or modulation periods (between 265 and 1,052 turns).[6] The preliminary results obtained so far do not add any new insight into the probelm but the importance of taking into account the modulating closed orbit, in addition to the modulating tunes, should be noted in the future investigations.

Acknowledgment

This study has been performed in its entirety at the Texas Accelerator Center (TAC) using its computing and other facilities. We are grateful to its director, Prof. F. Russ Huson, for his hospitalities throughout the duration of the work.

The particular version of TEAPOT used here was made available to us by Etienne Forest who shared his wisdom and expertise with us on many occasions. Alex Chao was generous in releasing many hours of his CRAY time to this study. We are grateful to them for their support.

References

1. P.L. Morton and J.F. Schonfeld, University of Michigan Report UM HE 84-1 (1984), p. 54.
2. Conceptual Design of the Superconducting Super Collider, SSC-SR-2020, March 1986, p. 202.
3. S. Heifets, University of Houston Report UH-IBPD-007-86 (1986).
4. L. Schachinger and R. Talman, SSC-52 (1985).
5. S. Chattopadhyay, Second Advanced ICFA Beam Dynamics Workshop, April 1988, Lugano, Switzerland.
6. J.L. Tennyson, SSC-155, January 1988.
7. J.C. Herrera, AIP Conference Proceedings No. 57 (1979), p. 29.
8. D.A. Edwards and L.C. Teng, IEEE.Trans. Nucl. Sci., NS-20 (1973), p. 885.
9. Ref. 2, section 4.5.7, p. 188.
10. Ref. 2, section 4.5.8, p. 189.

Appendix

Normalized rms emittance $\varepsilon_N = 1.0\times10^{-6}$m-rad,

rms emittance at 20 TeV $\varepsilon = 4.69\times10^{-11}$m-rad.

$$z \equiv x \text{ or } y$$

$$\sigma_z = \sqrt{\beta_z \varepsilon}\ , \quad (\text{amplitude})_z = \sqrt{\beta_z W_z} = \sqrt{\beta_z}\, A_z$$

$$(\text{av. amp.}/\sigma)_z = \bar{A}_z/\sqrt{\varepsilon} = 1.46\times10^5 \text{m}^{-\frac{1}{2}}\, \bar{A}_z$$

$$(r/\sigma) \equiv 1.46\times10^5 \text{m}^{-\frac{1}{2}} (\bar{A}_x^2 + \bar{A}_y^2)^{\frac{1}{2}}$$

Define $R \equiv (A_x^2 + A_y^2)^{\frac{1}{2}} \equiv (W_x + W_y)^{\frac{1}{2}}$,

$$\bar{R} = \sum_{i=1}^{N} (A_x^2 + A_y^2)_i^{\frac{1}{2}} / N \quad (\text{N=number of turns})$$

Then,

$$S_z = 2(A_z^{max} - A_z^{min})/(A_z^{max} + A_z^{min}),$$

$$S_{rms} = \{ \sum_{i=1}^{N} (R_i - \bar{R})^2/N \}^{\frac{1}{2}} / \bar{R}\ ,$$

$$C_{xy} = \frac{\Sigma (A_{xi} - \bar{A}_x)(A_{yi} - \bar{A}_y)}{\{\Sigma (A_{xi} - \bar{A}_x)^2\, \Sigma (A_{yi} - \bar{A}_y)^2\}^{\frac{1}{2}}}$$

where summations are from i = 1 to N (number of turns).

Table 3-1

Regular particle, Q_x = 78.265 (H) & 78.285 (V)

(av. amp./σ) (H)	(av. amp./σ) (V)	(r/σ)	fractional tunes (H)	fractional tunes (V)	S_x(%)	S_y(%)	S_{rms}(%)	C_{xy}
2.21	2.19	3.11	.2671	.2871	2.4	1.9	0.28	-0.25
4.40	4.47	6.28	.2679	.2875	6.8	5.8	0.71	-0.52
7.63	7.33	10.6	.2690	.2851	14.6	9.7	1.69	-0.33
8.31	7.89	11.5	.2692	.2847	15.5	12.8	1.97	-0.08
9.20	8.28	12.4	.26955	.2843	17.5	13.3	1.89	-0.20
10.1	9.44	13.8	.2700	.28405	14.6	10.7	1.57	-0.16
18.0	16.8	24.6	.2710	.2842	12.9	8.7	1.23	-0.19

Pacman particle

2.20	2.19	3.11	.2698	.2859	1.9	1.5	0.21	-0.22
4.39	4.44	6.25	.27005	.2861	4.6	4.4	0.46	-0.52
8.26	8.16	11.6	.2709	.2845	12.0	7.4	1.22	-0.28
10.8	10.3	14.9	.27135	.2842	16.4	7.9	2.52	+0.29
12.7	11.2	17.0	.2715	.2842	26.8	10.0	4.68	+0.56
17.4	17.3	24.6	.2717	.2843	15.0	7.1	1.88	+0.15

Table 3-2

Regular particle, Q_x = 78.267 (H) & 78.287 (V)

4.45	4.47	6.32	.2700	.2895	8.0	6.4	0.72	-0.54
6.03	5.99	8.50	.2704	.2882	12.3	10.9	1.27	-0.50
8.37	7.35	11.1	.2714	.2869	37.2	12.4	5.91	+0.40
9.70	10.9	14.6	.2719	.2860	45.3	42.8	7.92	+0.30

Pacman particle

4.40	4.49	6.28	.2720	.28805	4.6	5.5	0.56	-0.40
5.88	5.96	8.37	.2724	.2874	7.5	6.4	0.70	-0.56
8.94	8.83	12.6	.2730	.2862	8.8	9.5	1.25	-0.08
10.5	10.3	14.7	.2733	.2861	8.7	12.6	1.65	-0.33

Regular particle, Q_x = 78.263 (H) & 78.283 (V)

4.41	4.47	6.28	.2659	.28545	6.7	5.6	0.73	-0.50
5.96	6.02	8.47	.2662	.2842	12.1	9.6	1.25	-0.55
7.81	7.36	10.7	.2671	.2829	17.5	11.0	1.50	-0.50
10.3	10.8	14.9	.2681	.28175	15.4	25.2	2.58	-0.49

Pacman particle

4.40	4.45	6.25	.2681	.28405	5.0	4.0	0.46	-0.52
5.93	5.97	8.42	.2684	.2833	9.9	6.3	0.95	-0.36
9.04	8.89	12.7	.2690	.2822	12.8	9.4	1.61	+0.27
10.4	10.1	14.5	.2692	.2822	15.3	11.5	2.19	+0.01

Table 3-3

Regular particle, (av. amp./σ) ≈ 4 for both directions.

	Case 1	Case 2	Case 3	Case 4	Case 5
S_x(%)	6.8	6.2	7.1	6.4	6.6
S_y(%)	5.8	5.8	6.4	6.3	6.3
S_{rms}(%)	0.71	0.70	0.79	0.75	0.69
C_{xy}	-0.52	-0.50	-0.43	-0.45	-0.53

Regular particle, (av. amp./σ) ≈ 10 for both directions.

	Case 1	Case 2	Case 3	Case 4	Case 5
S_x(%)	29.0	30.5	33.2	NA	29.8
S_y(%)	22.7	22.6	22.6		14.0
S_{rms}(%)	2.29	2.71	3.61		3.17
C_{xy}	-0.80	-0.76	-0.67		-0.67

Pacman particle, (av. amp./σ) ≈ 4 for both directions.

	Case 1	Case 2	Case 3	Case 4	Case 5
S_x(%)	4.6	3.9	4.6	4.4	4.3
S_y(%)	4.4	4.3	4.5	4.8	4.7
S_{rms}(%)	0.46	0.46	0.56	0.52	0.49
C_{xy}	-0.52	-0.51	-0.40	-0.42	-0.50

Pacman particle, (av. amp./σ) ≈ 10 for both directions.

	Case 1	Case 2	Case 3	Case 4	Case 5
S_x(%)	16.4	16.0	NA	17.0	16.2
S_y(%)	7.9	7.4		7.9	7.3
S_{rms}(%)	2.52	2.09		2.69	2.35
C_{xy}	+0.29	+0.20		+0.32	+0.29

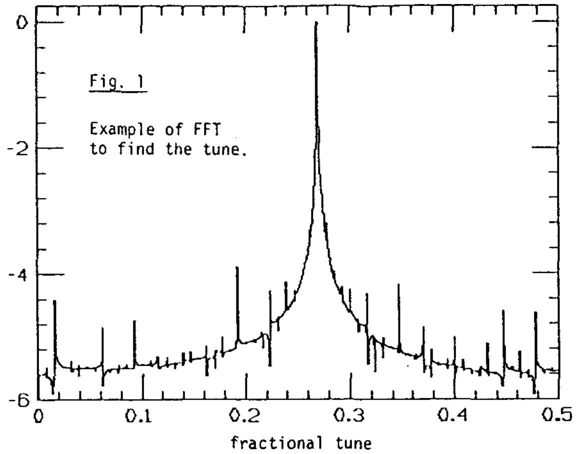
Fig. 1
Example of FFT
to find the tune.
0
-2
-4
-6
0
0.1
0.2
0.3
0.4
0.5
fractional tune

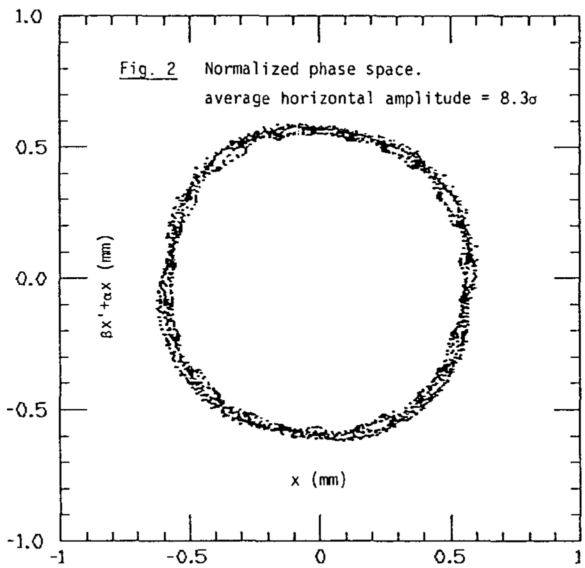
Fig. 2
Normalized phase space.
average horizontal amplitude = 8.3σ
1.0
0.5
0.0
-0.5
-1.0
βx'+αx (mm)
-1
-0.5
0
0.5
1
x (mm)

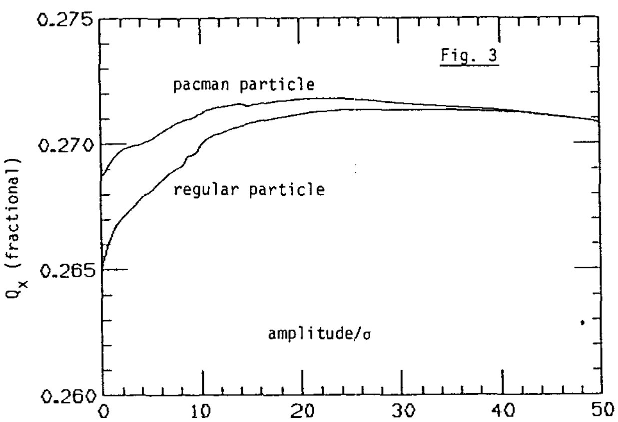
Fig. 3
pacman particle
regular particle
0.275
0.270
0.265
0.260
Qx (fractional)
0
10
20
30
40
50
amplitude/σ

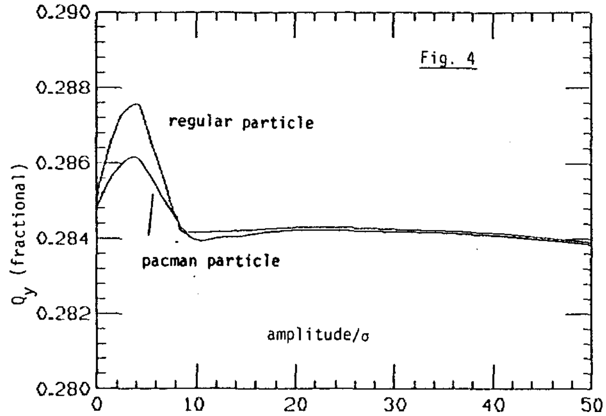
Fig. 4
regular particle
pacman particle
0.290
0.288
0.286
0.284
0.282
0.280
Qy (fractional)
0
10
20
30
40
50
amplitude/σ

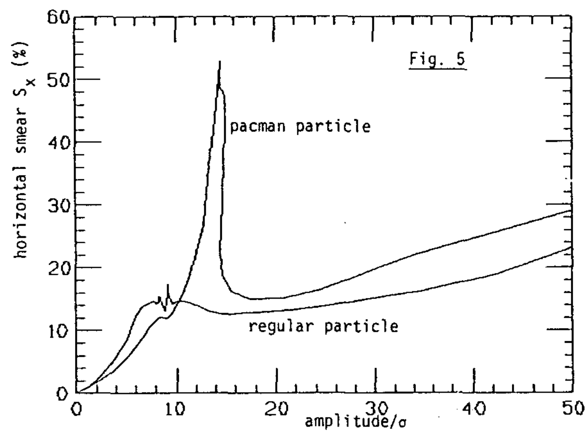
Fig. 5
pacman particle
regular particle
60
50
40
30
20
10
0
horizontal smear Sx (%)
0
10
20
30
40
50
amplitude/σ

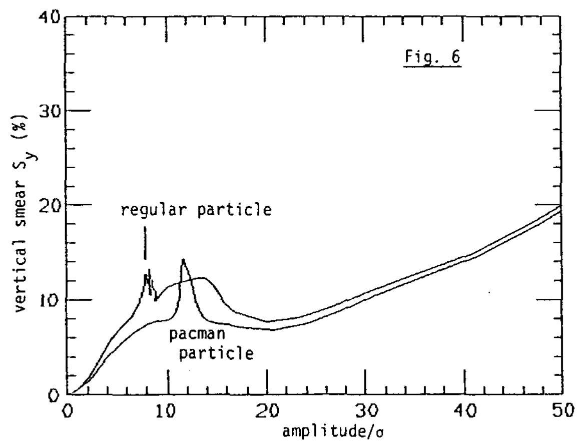
Fig. 6
regular particle
pacman
particle
40
30
20
10
0
vertical smear Sy (%)
0
10
20
30
40
50
amplitude/σ

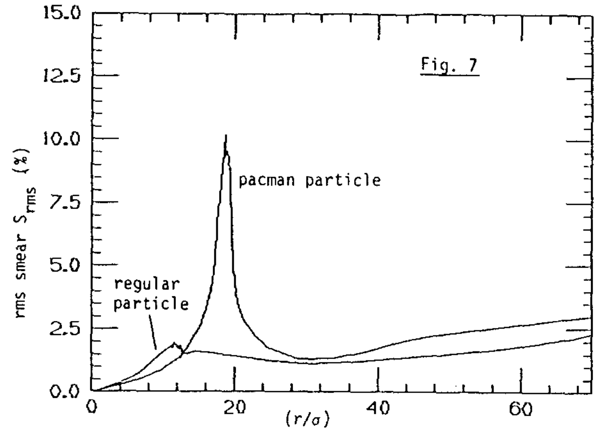
Fig. 7
pacman particle
regular
particle
rms smear S_{rms} (%)
(r/σ)
0.0
2.5
5.0
7.5
10.0
12.5
15.0
0
20
40
60

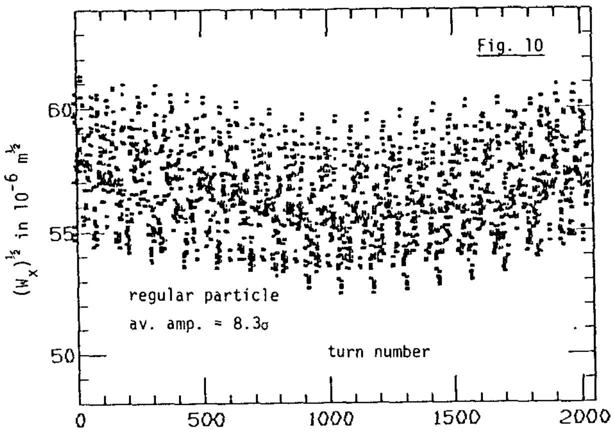
Fig. 10
regular particle
av. amp. = 8.3σ
turn number
$(W_x)^{1/2}$ in 10^{-6} $m^{1/2}$
50
55
60
0
500
1000
1500
2000

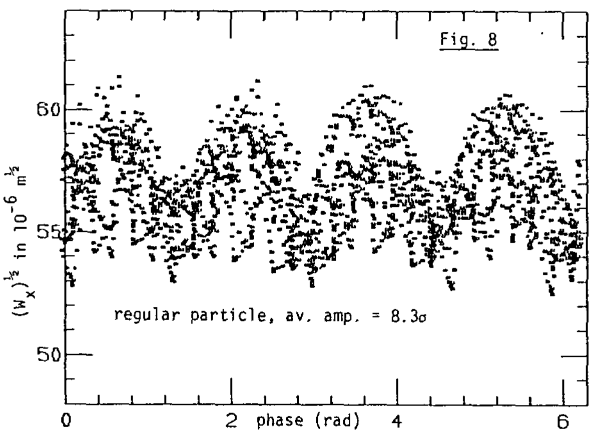
Fig. 8
regular particle, av. amp. = 8.3σ
$(W_x)^{1/2}$ in 10^{-6} $m^{1/2}$
phase (rad)
50
55
60
0
2
4
6

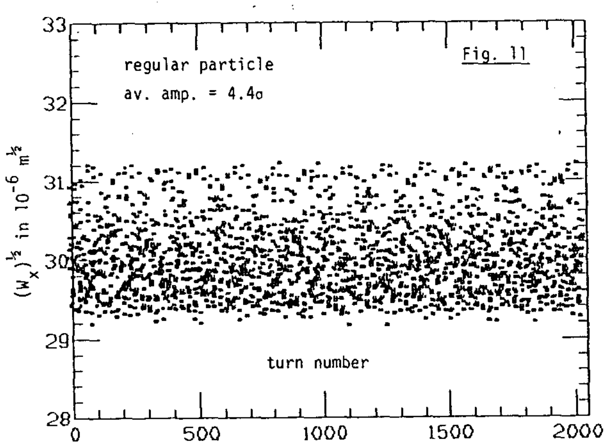
Fig. 11
regular particle
av. amp. = 4.4σ
turn number
$(W_x)^{1/2}$ in 10^{-6} $m^{1/2}$
28
29
30
31
32
33
0
500
1000
1500
2000

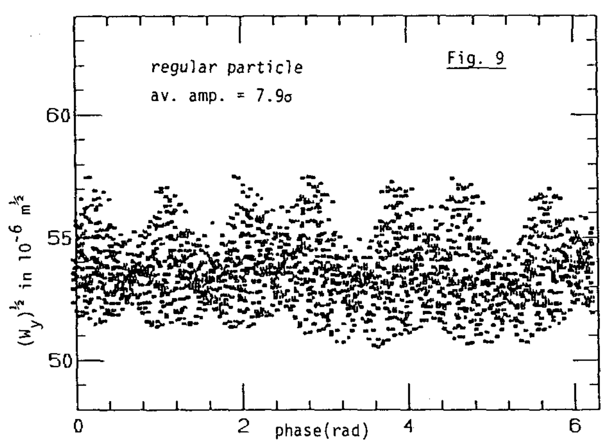
Fig. 9
regular particle
av. amp. = 7.9σ
$(W_y)^{1/2}$ in 10^{-6} $m^{1/2}$
phase(rad)
50
55
60
0
2
4
6

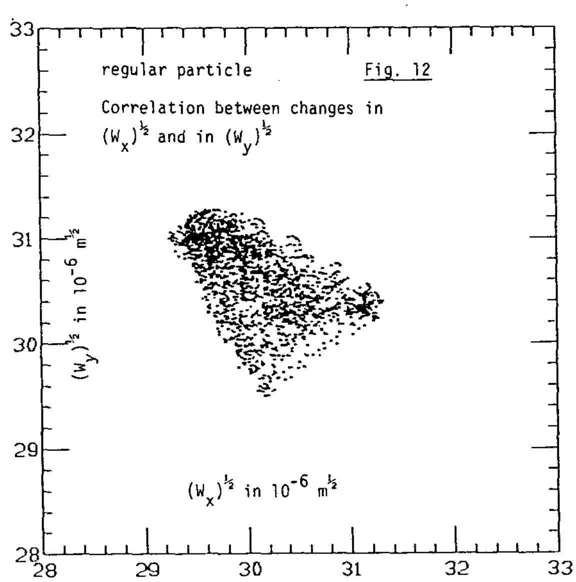
regular particle
Fig. 12
Correlation between changes in
$(W_x)^{1/2}$ and in $(W_y)^{1/2}$
$(W_y)^{1/2}$ in 10^{-6} $m^{1/2}$
$(W_x)^{1/2}$ in 10^{-6} $m^{1/2}$
28
29
30
31
32
33
28
29
30
31
32
33

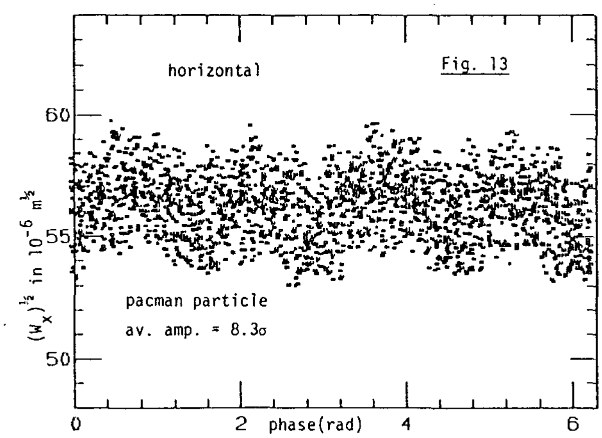
Fig. 13
horizontal
pacman particle
av. amp. = 8.3σ
$(W_x)^{1/2}$ in 10^{-6} $m^{1/2}$
phase(rad)
60
55
50
0
2
4
6

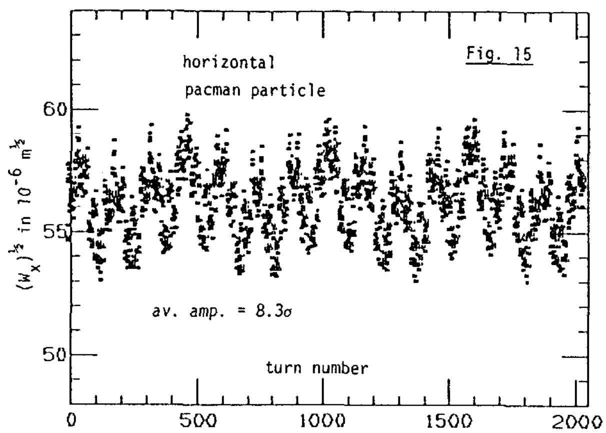
Fig. 15
horizontal
pacman particle
av. amp. = 8.3σ
turn number
$(W_x)^{1/2}$ in 10^{-6} $m^{1/2}$
60
55
50
0
500
1000
1500
2000

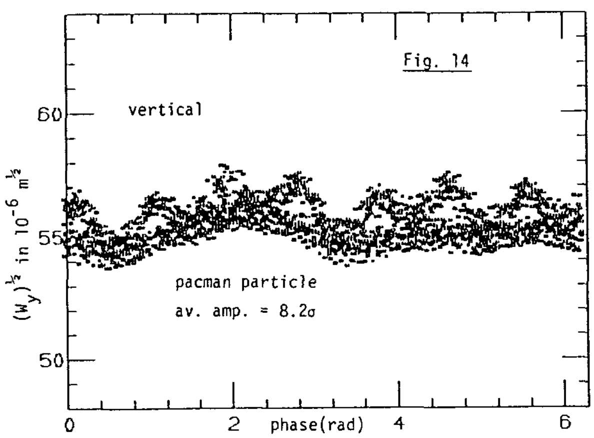
Fig. 14
vertical
pacman particle
av. amp. = 8.2σ
$(W_y)^{1/2}$ in 10^{-6} $m^{1/2}$
phase(rad)
60
55
50
0
2
4
6

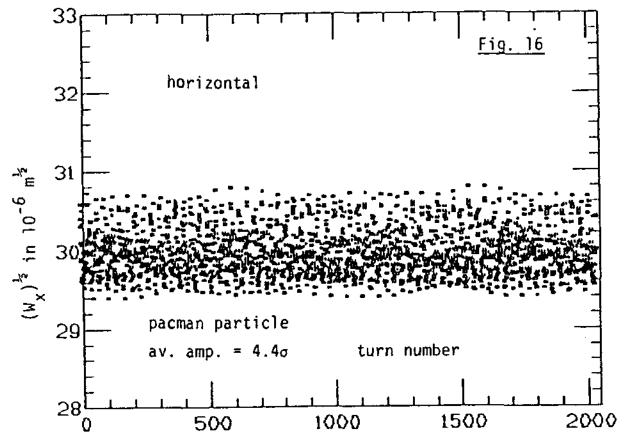
Fig. 16
horizontal
pacman particle
av. amp. = 4.4σ
turn number
$(W_x)^{1/2}$ in 10^{-6} $m^{1/2}$
33
32
31
30
29
28
0
500
1000
1500
2000